Journal of Applied Sciences

ISSN 1812-5654

science alert

ANSInet
an open access publisher
http://ansinet.com

Journal of Applied Sciences 13 (6): 854-861, 2013
ISSN 1812-5654 / DOI: 10.3923/jas.2013.854.861

Test System and Model for Fatigue Performance Evaluation of Marine Riser

[1]Wang Chuan, [1]Hongwu Zhu and [2]Dingya Wang
[1]College of Mechanical and Transportation Engineering, China University of Petroleum, Beijing, 102249, China
[2]CNPC Baoji Oilfield Machinery Co., LTD, Baoji, 721002, China

Abstract: Marine risers that connect the surface floating facilities and the subsea wells are generally made of heavy duty girth welded tubulars. When experience dynamic loads, weld defects can cause the marine risers to fail prematurely due to fatigue cracks initiation. In order to investigate the fatigue performance of marine risers, a fatigue test system was designed. The components of the test setup part and the data measurement part were described. A mathematical model of free massive beam is built to find the natural frequencies and natural modes of the testing specimen of marine riser to guide the test. Adding end masses is an effective method to control the natural modes and stress amplitude. Based on this system, the fatigue performance of a specimen of marine riser with flange joint is evaluated and the principle and process of the test were illustrated. The mathematical model was used to predict the lateral displacement and the bending moment of the excitated specimen. The maximum error between the test and the theoretical results of bending stress is +4.93%, which verified the model. This study brought promotional values for fatigue performance evaluation of marine risers with different welded tubulars and connections.

Key words: Marine riser, fatigue, natural frequency, excitation, mathematical model

INTRODUCTION

As important structural members offshore, marine risers that connect the surface floating facilities and the subsea wells are generally made of heavy duty girth welded tubulars. These girth welds are often the key parts and the limiting factor in marine risers design. As fracture critical components, marine risers require high performance reliability due to the unacceptable consequences caused by any potential failure. For this reason, fatigue test on marine risers is important to examine their performance.

Over the past years, several fatigue test methods have been used to evaluate the fatigue life of marine risers in different ways. Axial tension fatigue test can directly find out the stress according to the sections and axial load of specimen to validate the performance of material, but cannot work for the full scale specimen (McMaster *et al*., 2007). The process of the four-point bending test is simple, but lasts a long testing time with low efficiency (Van Wittenberghe *et al*., 2011). The Resonant Translational Bending (RTB) technique was proven as a quick and efficient method of fatigue performance evaluation for girth welds and mechanical joints in tubing pipe, casing pipe and drilling pipe (Kerkhof *et al*., 1990; Varma *et al*., 1997) and is going to be a trend to test marine risers for economical and efficiency reasons (Buitrago *et al*., 2003). But the previous works still have left unresolved issues: (1) These works mainly focused on the fatigue test results analysis (Hasegawa *et al*., 2002; Varma *et al*., 2002). The principle and process of RTB test was barely mentioned; (2) A finite element model was generally used to predict and guide the test (Bertini *et al*., 2008), did not study the relationship between the relative parameters in different test conditions, such as the effect of end mass on the natural frequencies of testing specimen.

In this study, a fatigue test was performed on a marine riser with flange joint. The fatigue test system which produces a resonant translational bending consisting of a test setup part and a data measurement part was described. A mathematical model was built to control and obtain the required natural frequencies and the response of testing specimen to guide towards the test execution. Furthermore, this article has a greater promotional value for design of fatigue test system and test of other marine risers.

FATIGUE TEST SYSTEM DESIGN

The fatigue test system was based on the principle of resonant translational bending. In order to produce

Corresponding Author: Wang Chuan, College of Mechanical and Transportation Engineering, China University of Petroleum, Beijing, 102249, China Tel: +8601089733749

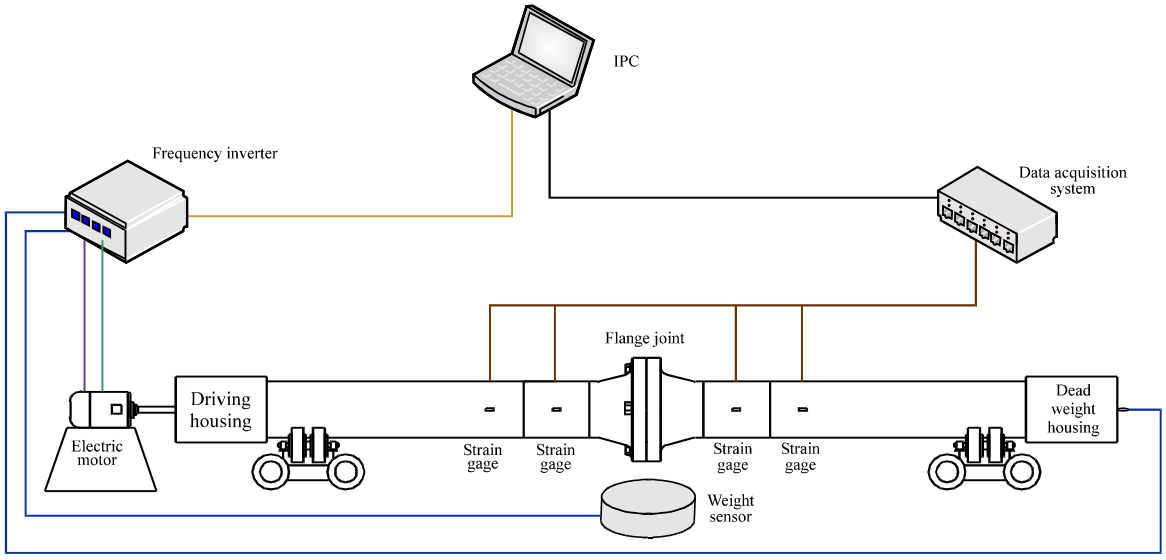

Fig. 1: Layout of fatigue test setup of marine riser

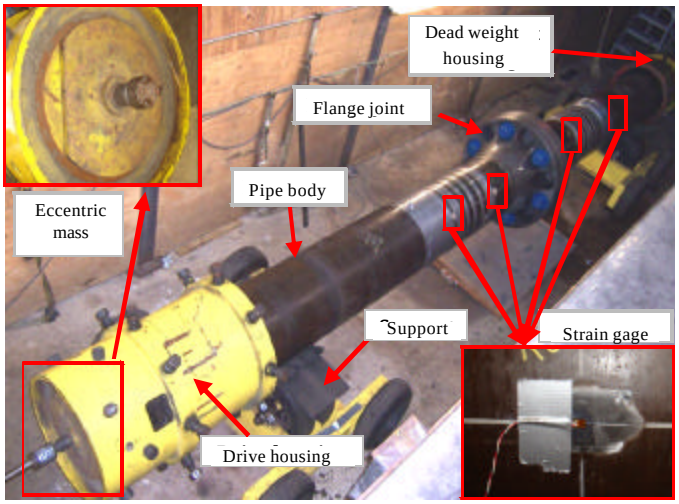

Fig. 2: Components of test setup part

enough bending load to meet the test condition, a testing specimen of marine riser consists of two long pipe bodies, one mid-joint (in this study is the flange joint) and welds. During test, the specimen was applied an excitation with a frequency close to its natural frequency, which causes the specimen come into resonance. As shown in Fig. 1, the fatigue test system consists of a setup part and a data measurement part.

Test setup: An overview of the test setup is shown in Fig. 2. The specimen is supported by two supports. The drive housing is clamped to one end of the specimen, in which a rotating eccentric mass connected to the variable speed electromotor driven via a cardan shaft. The electromotor is used to generate the frequency of excitation. It drives the eccentric mass to load the specimen near its first natural frequency by adjusting its RPM. Eccentricity of the eccentric mass plays an important role to create and control excitation force. The dead weight housing is clamped to the other end of the specimen to balance the assembly. Both the housings can be changed to be applicable for the marine risers with

different diameters and wall thicknesses. As the eccentric mass is replaceable, some eccentric masses with different weight and eccentricity were prefabricated to meet a wide range of test requirement.

Data measurement: The data measurement system consists of strain gages, Industrial Personal Computer (IPC), Uninterrupted Power Supply (UPS), data acquisition software, frequency inverter, weight sensor, pressure switch, as shown in Fig. 1. Axial strain gages on the outer surface of the pipe body are used to monitor the bending strains during test. Both bending strains and number of cycles are monitored and recorded by the data acquisition software which could obtain 16 groups data at the same time. Each minute the data acquisition software records the average maximum and minimum strains for each strain gage along with the number of cycles. The weight sensor is placed below the flanges to stop the test if a bolt fails and drops out of the flange. When the internal pressure drops due to a through-wall crack, the pressure switch installed on the dead weight housing will stop the test. Frequency inverter is used to provide power to electromotor and control its output frequencies to meet test condition. As long last the test, even one day, a UPS is used to provide emergency power to ensure continuity of the test.

Specimen for modeling and test: In order to explain the principle and process of test conveniently, a specimen of marine riser with flange joint will be modeled and tested. As Fig. 3 shows, the total length of the specimen is about 8229.6 mm. Its Outer Diameter (OD) and Internal Diameter (ID) are 533.4 and 501.6 mm, respectively. Its weight is 2590 kg. The specimen contains a made up flange joint in center, two pipe-to-pipe welds (W1, W4) and two flange-to-riser pipe welds (W2, W3). The purpose of the test is to evaluate the fatigue performance of welds undergo the same load cycle during one excitation cycle. Because the weld and wall mismatch will cause local distorted strains, the gages should be placed far enough from the welds to obtain pipe body stresses. Four sections (S1 to S4) are located on either side of the welds. Sixteen strain gages are installed on circumferential locations 0°, 90°, 180° and 270° around the pipe body at each section. The test will be performed at room temperature within about 30 Hz at the specified stress range resulting in 1.7-2.5 million cycles a day.

MATHEMATICAL MODEL

Fundamental equations: In RTB test, the specimen is applied an excitation by a typical electromotor with about 20 to 40 Hz range of frequency. Because of its long size, the natural frequency (generally is above 40 Hz) of the specimen is difficult to get within the frequency range of electromotor. The natural frequency mainly depends on bending stiffness and mass. Therefore, the natural frequencies of specimen can be lowered by attaching proper masses at both ends of the pipe body. In this work, the drive housing and dead weight housing were used as end mass.

The specimen was assumed to be a model of free massive beam (with total mass m_s uniformly distributed on the length L, two masses m_f at both ends of the riser pipe, l_b the distance from the centers (x direction) of end masses to the riser pipe ends) to calculate its natural frequencies and natural modes, as shown in Fig. 4.

The dynamic behavior of the specimen can be expressed using a partial differential equation:

$$EI\frac{\partial^4 u(x,t)}{\partial x^4}+\frac{m_s}{L}\cdot\frac{\partial^2 u(x,t)}{\partial t^2}=0 \quad (1)$$

where, u(x,t) is the lateral displacement of the specimen, E is Young's modulus, I is area moment of inertia and m_s/L is the mass per meter of the specimen.

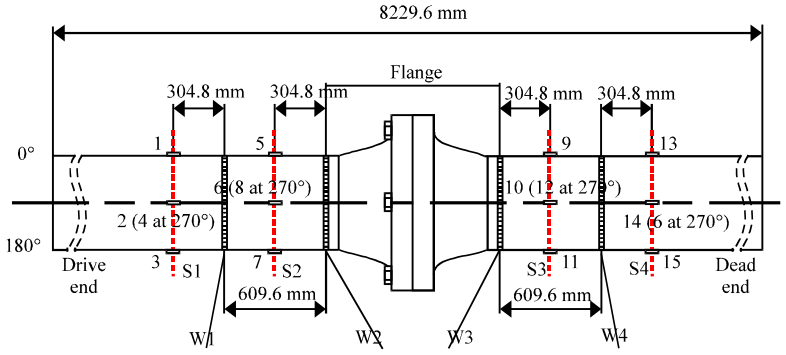

Fig. 3: Location of strain gages and welds

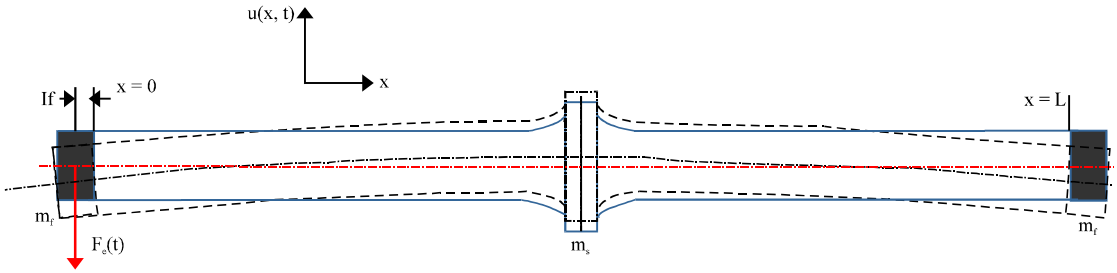

Fig. 4: Dynamic model of a free massive beam

By solving this partial differential equation, the general solution of Eq. 1 can be written as Eq. 2:

$$u(x, t) = X(x)e^{i\omega t} \quad (2)$$

where, X(x) can be given by Eq. 3 with arbitrary constants A_1, A_2, A_3, A_4 and λ which is written as Eq. 4:

$$X(x) = A_1 \cos(\lambda x)+A_2 \sin(\lambda x) + A_3 \cosh(\lambda x)+A_4 \sinh(\lambda x) \quad (3)$$

$$\lambda = \sqrt[4]{\frac{m_s}{EIL}\omega^2} \quad (4)$$

In order to obtain the arbitrary constants, boundary conditions at of the specimen ends are substituted into the partial differential equation, as shown from Eq. 5-7:

$$x = 0 \quad \begin{cases} EI\dfrac{\partial^2 u}{\partial x^2} + m_f l_f \cdot \dfrac{\partial^2 u}{\partial t^2} - (J_f + m_f l_f)\cdot \dfrac{\partial^3 u}{\partial x \partial t^2} = F_e l_f \\ EI\dfrac{\partial^3 u}{\partial x^3} + m_f \cdot \dfrac{\partial^2 u}{\partial t^2} - m_f l_f \cdot \dfrac{\partial^3 u}{\partial x \partial t^2} = F_e \end{cases} \quad (5)$$

$$F_e = m_e r_e \omega_e^2 e^{i\omega_e t} \quad (6)$$

$$x = L \quad \begin{cases} EI\dfrac{\partial^2 u}{\partial x^2} + m_f l_f \cdot \dfrac{\partial^2 u}{\partial t^2} + (J_f + m_f l_f)\cdot \dfrac{\partial^3 u}{\partial x \partial t^2} = 0 \\ -EI\dfrac{\partial^3 u}{\partial x^3} + m_f \cdot \dfrac{\partial^2 u}{\partial t^2} + m_f l_f \cdot \dfrac{\partial^3 u}{\partial x \partial t^2} = 0 \end{cases} \quad (7)$$

where, J_f is the mass moment of inertia of end mass, $F_e(t)$ is an excitation force caused by spinning the eccentric mass me in the drive housing. It will induce rotating bending with high amplification near the resonance and can be written as Eq. 6, where r_e is the eccentricity of rotating mass and ω_e is the angular excitation frequency. In the boundary conditions, $EI\partial^2 u/\partial x^2$, $m_f l_f \partial^2 u/\partial t^2$ and $(J_f+m_f l_f)\partial^3 u/\partial x \partial t^2$ are the bending moments of the specimen, linear acceleration motion of m_f and angular acceleration motion of $m_f$respectively, $EI\partial^3 u/\partial x^3$, $m_f \partial^2 u/\partial x^2$, $m_f l_f \partial^3 u/\partial x \partial t^2$ are the corresponding shear forces.

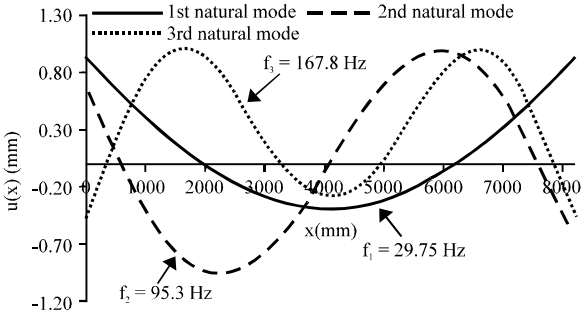

Fig. 5: The first three nature modes of the free massive beam

Control of natural frequency: When $F_e(t) = 0$, the angular natural frequencies ω_n and natural modes are found. In Fig. 5, the first three nature frequencies and corresponding nature modes of the specimen are calculated by Matlab™ ver. 7.01, where $f = \omega/2\pi$, E = 201Gpa, m_s = 2590 kg, m_f =210 kg, l_f = 60.25 mm.

When $F_e(t) = 0$ and $m_f = 0$, the first natural frequencies and natural modes of the specimen without end mess can also be found to analyze the effect of end mess. As shown in Fig. 6, adding end mass is an effective way to affect the first natural model of the specimen. With 210 kg end mess, the maximum lateral displacement of the specimen increased from 0.72 to 0.85 mm and the first natural frequency of the specimen is controlled from 40.52 Hz down to 29.75 Hz, which meets the test condition of about 30 Hz. This indicates that the attached end masses can improve the excitation efficiency and the reduction of the natural frequencies of the specimen produced by the end masses is particularly remarkable.

As the specimen is assumed to a free massive beam, no constraint condition is applied. The specimen will be simply supported by two supports. In Fig. 6, it is found

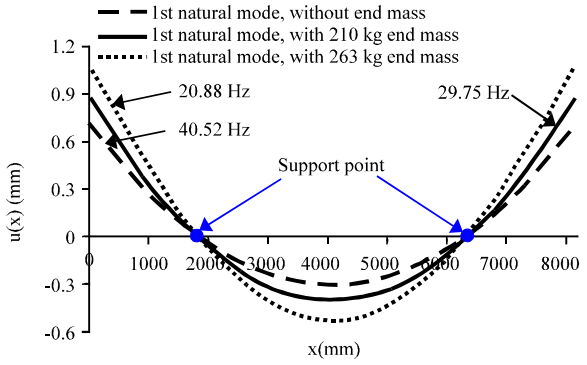

Fig. 6: Effect of end mess on the first natural mode of the specimen

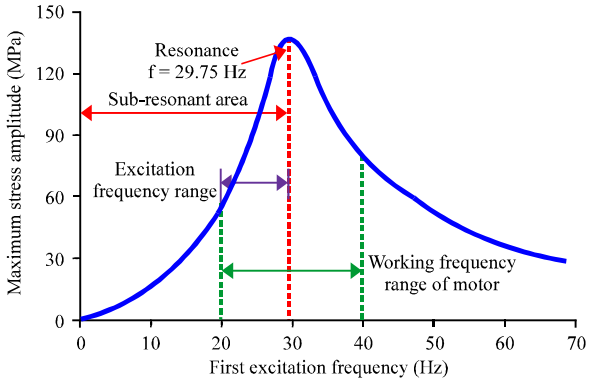

Fig. 7: Excitation frequency range induced by resonance

that even the weight of end mass is increased from 0 kg up to 263 kg continuously, the location of the two null displacement points will never change. Therefore, the supports will be located at the two points where lateral displacement is null.

Control of natural frequency: When the angular excitation frequency ω_e (close to ω_n), m_e and r_e are chosen, lateral displacement of the specimen can be calculated by Eq. (8):

$$u(x,t) = X_n(x)e^{i\omega_e t} \tag{8}$$

where, ω_e is the rotational speed of eccentric masses generated by electromotor and could be expressed by excitation frequency f_e. The bending moment M(x) and the resulting stress $\sigma_B(x)$ at the outer surface of the specimen can be written by Eq. 9 and 10:

$$M(x) = EI\frac{d^2X_n(x)}{dx^2} \tag{9}$$

$$\sigma_B(x) = \frac{ED}{2}\cdot\frac{d^2X_n(x)}{dx^2} \tag{10}$$

In the mathematical model, no damping effect is considered. Based on this assumption, the excitation frequency should be equal to the natural frequency of the specimen. However, when the excitation frequency moves up on the resonance status, the damping effect on the test results becomes more significant and results in a strongly amplified in practice. Therefore, the excitation frequency should be chosen within an overlap area of sub-resonant area of the specimen and working frequency range of the electromotor. In Fig. 7, the maximum theoretical bending stress of the specimen (at the mid-joint) is calculated by Eq. 10 and is plotted versus the first excitation frequency. For the specimen with 210 kg end mass, the excitation frequency range is chosen between 20 and 30 Hz. As the natural frequency of specimen is 29.75 Hz, the excitation frequency should be closed to it. If the stress amplitude requires a value of 120 MPa, the excitation frequency is chosen with about 27.5 Hz.

TEST RESULTS AND ANALYSIS

Verification of mechanical model: In Fig. 8, the lateral displacement and bending moment of the excitated specimen by electromotor are predicted by Eq. 8 and 9, respectively. With m_e = 35.8 kg, r_e = 33 mm, the lateral displacement has an amplitude of 0.38 mm and the bending moment reaches a value of 436 kNm at the flange joint. The location x = 1830 mm and x = 6360 mm are the point where the specimen should be supported in the test system.

In the RTB test, a 28.2 Hz excitation frequency that was about 0.95 times the natural frequency of the specimen generated by electromotor. Figure 9 shows the theoretical and test results of bending stress at the OD of specimen, on which the stress distribution along the specimen was calculated by Eq. 10. Test results are the mean value at section S1, S2, S3 and S4 (with 4 strain gages at one section). The bending stress developed in the specimen are close to zero at the ends and reaches about 136.5 MPa at the flange joint. The maximum theoretical stress of welds is 124.1 MPa at W3. Among the four sections, the maximum error is +4.93% at S4. From S1 to S4, the relative error increases continuously, as shown in Table 1. The reason could be that (1) The specimen is simply supported by two couples of rubber wheels (Fig. 2). The friction at the supporting wheels will affect

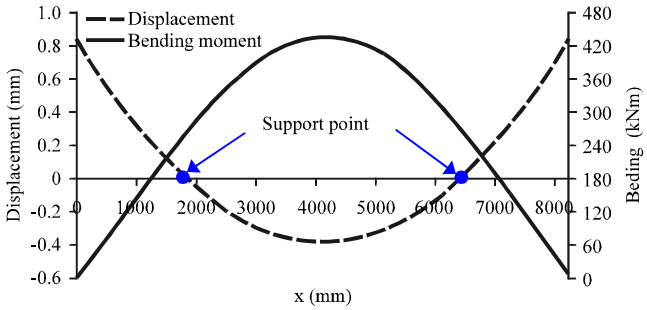

Fig. 8: Displacement and bending moment with excitation

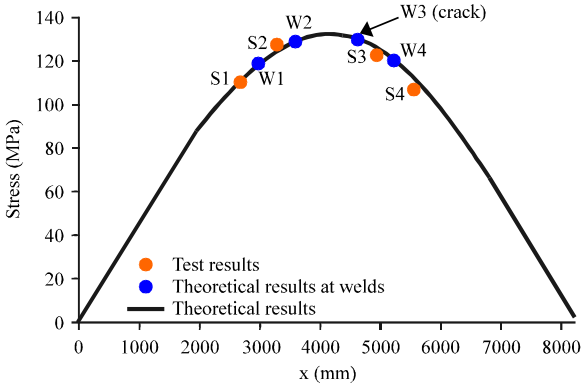

Fig. 9: The theoretical and test bending stress at the OD of specimen

the excitation from electromotor. When the excitation frequency moves up to the natural frequency of the specimen, this influence will be strongly amplified and (2) The excitation is transmitted from S1 to S4, which accumulates the relative error of the four sections. The theoretical results are accurate and agree very well with the test results. It can be concluded that theoretical results at the four sections were verified through strain gauges measurements during tests and the mathematical model could satisfactorily calculate the behaviors of the specimen applied an excitation.

In Fig. 10, the stress amplitude of the sixteen strain gauge locations over time is shown. The vibration direction of strain gauge location is in z-direction on 0° and 180° and is in y-direction on 90° and 270°. It can be seen that the y-stress and z-stress have the almost equal amplitude at the same section, but that the y-stress has a phase delay of 90°. This means that the standing wave of excitation transmitted in a clockwise circular direction.

Fatigue curve for marine risers: The fatigue design is based on the use of S-N curves, which are obtained from

Table 1: Comparison between theoretical and test results

Monitors	S1	S2	S3	S4
Test results (MPa)	110.30	127.26	122.96	107.50
Theoretical results (MPa)	111.50	124.82	125.71	112.80
Relative error* (%)	+1.08	-1.93	+2.24	+4.93

*Relative error = (Theoretical results-test results)/test results×100%

fatigue tests. Fatigue curves specifically for marine risers have not yet been adopted. However, fatigue curves published by BSI (1993) and DET NORSKE VERITAS (DNV, 1984) for offshore structures have been used to design and assess the fatigue performance of marine risers. Single sided girth welds such as those used for marine riser fabrication are generally classified as F2 for the purpose of fatigue analysis. A survey of a wide range of test results on single sided girth welds (Dickerson, 1997) shows that in almost all cases the performance of the welds exceeds that of an E fatigue detail classification (BSI, 1993; DNV, 1984). This gives a fatigue resistance some 2 to 3 times that of an F2 curve. The weld test specimens considered are representative of welds used for pipeline construction. Riser welds are expected to be as good if not of better quality than those of the weld test specimens reviewed. Based on this review, it is reasonable that as an E-class fatigue detail is used for the fatigue life prediction of marine riser coupling welds and an F2-class fatigue detail is used for the fatigue test.

Test results: The specimen was tested twice. The W3 weld cracked after 316,306 cycles. The crack ground out with the length of about 52 mm until it was no longer visible, as shown in Fig. 11. After patching the crack by repairing welding, the specimen was loaded back into the test system and cycled at the original stress range until it cracked at the repair weld and leaked after a total of 442,637 cycles (including the initial 316,306 cycles). In Fig. 12, the test results are presented and superimposed on the design fatigue curves of E and F2 in BS7608 of BSI. The fatigue results of the cracked W3 weld are plotted in the S-N curve. The pipe-to-flange weld W3 did not pass

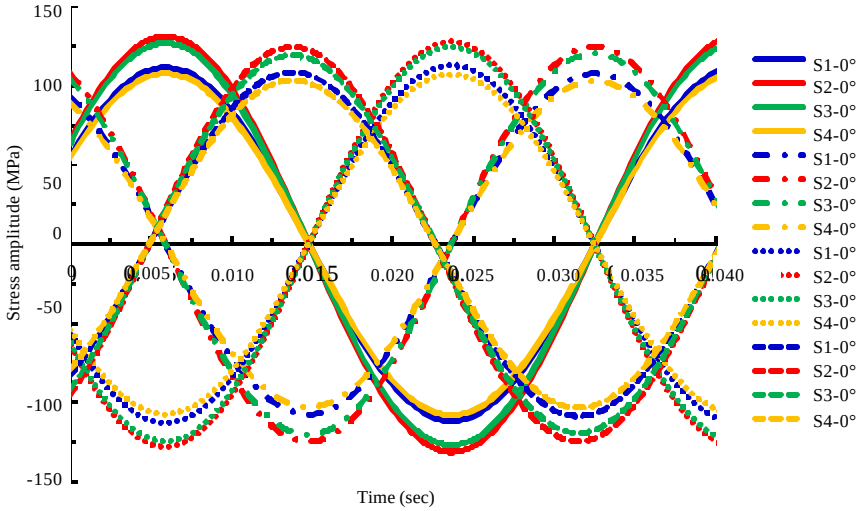

Fig. 10: Stress amplitude of strain gauge locations

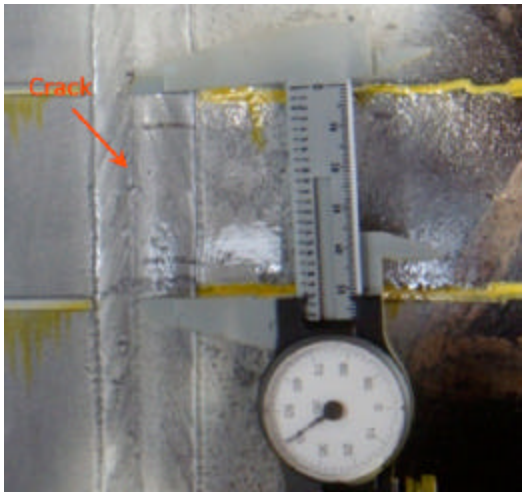

Fig. 11: Crack on W3 weld of the specimen

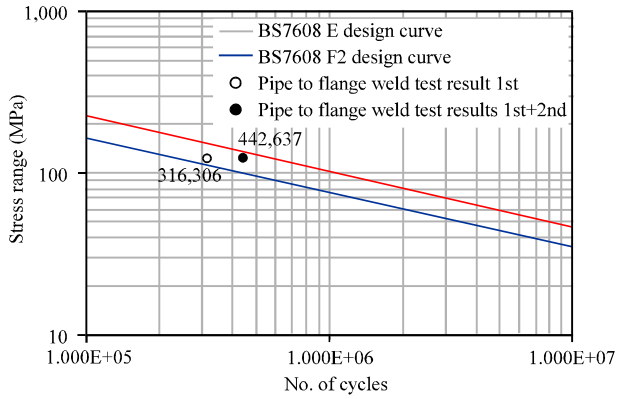

Fig. 12: Marine riser fatigue test results

the E design curve but passed the target life of F2 design curve, indicating that the cracked weld is of generally acceptable quality and meets the design requirements, but its fatigue life could not satisfy the test requirements.

CONCLUSION

A RTB test system consists of the setup part and data measurement part was established. A mathematical model was built to guide test. End mass is an important effect factor to control natural frequencies of the specimen to meet the test condition. Based on this test system, the fatigue performance of a specimen with flange joint was evaluated. Both theoretical and test results could obtain the bending stress distribution characteristics on the outer surface of the specimen with a good agreement. The specimen cracked at pipe-to-flange weld W3 with about 124.1 Mpa stress. This study is also bringing promotional values for other marine risers with different tubulars and connections.

REFERENCES

BSI, 1993. BS 7608: Fatigue design and assessment of steel structures. British Standards Institute (BSI), British.

Bertini, L., M. Beghini, C. Santus and A. Baryshnikov, 2008. Resonant test rigs for fatigue full scale testing of oil drill string connections. Int. J. Fatigue, 30: 978-988.

Buitrago, J., M.S. Weir and W.C. Kan, 2003. Fatigue design and performance verification of deepwater risers. Proceedings of the International Conference on Offshore Mechanics and Arctic Engineering, June 8-13, 2003, Cancun, ASME, pp: 351-366.

Dickerson, T.L., 1997. Guidance on fatigue and fracture aspects of welded joints in catenary risers. TWI Report, Cambridge.

DnV, 1984. Classification note 30.2: Fatigue strength analysis of mobile offshore units. Det Norske Veritas (DnV), Norway.

Hasegawa, K., K. Sakata, K. Miyazaki and S. Kanno, 2002. Fatigue strength for pipes with allowable flaws and design fatigue curve. Int. J. Pressure Vessels Piping, 79: 37-44.

Kerkhof, K., W. Stoppler, D. Sturm and R. Zirn, 1990. Resonant excitation of a pipe section. Nuclear Eng. Des., 119: 361-370.

McMaster, F., J. Bowman, H. Thompson, M. Zhang and S. Kinyon, 2007. Sour service corrosion fatigue testing of flowline welds. Proceedings of the International Conference on Offshore Mechanics and Arctic Engineering, June 10-15, 2007, ASME, San Diego, pp: 27-35.

Van Wittenberghe, J., P. De Baets, W. De Waele, T.T. Bui and G. De Roeck, 2011. Evaluation of fatigue crack propagation in a threaded pipe connection using an optical dynamic 3D displacement analysis technique. Eng. Failure Anal., 18: 1115-1121.

Varma, A.H., A.K. Salecha, B. Wallace and B.W. Russell, 2002. Flexural fatigue behavior of threaded connections for large diameter pipes. Exp. Mechanics, 42: 1-7.

Varma, A.H., B.W. Russell and B. Wallace, 1997. Large-scale rotating bending fatigue tests for offshore pipe connections. Exp. Mech., 37: 147-153.